Acta Crystallographica Section F
Structural Biology and Crystallization Communications
ISSN 1744-3091

The structure of LpxD from *Pseudomonas aeruginosa* at 1.3 Å resolution

John Badger,[a]* Barbara Chie-Leon,[a] Cheyenne Logan,[a] Vandana Sridhar,[a] Banumathi Sankaran,[b] Peter H. Zwart[b] and Vicki Nienaber[a]

[a]Zenobia Therapeutics, 505 Coast Boulevard South, Suite 111, La Jolla, CA 92122, USA, and [b]Berkeley Center for Structural Biology, Physical Biosciences Division, Lawrence Berkeley Laboratory, 1 Cyclotron Road, BLDG 6R2100, Berkeley, CA 94720, USA

Correspondence e-mail: john@zenobiatherapeutics.com

Received 12 April 2011
Accepted 17 May 2011

PDB Reference: LpxD, 3pmo.

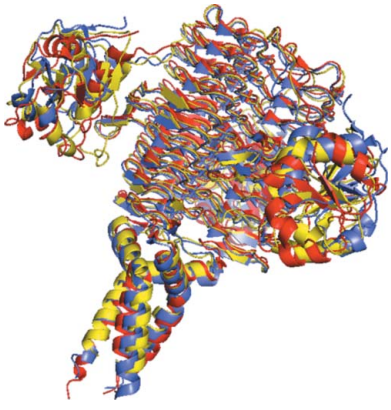

LpxD is a bacterial protein that is part of the biosynthesis pathway of lipid A and is responsible for transferring 3-hydroxymyristic acid from the *R*-3-hydroxymyristoyl-acyl carrier protein to the 2-OH group of UDP-3-*O*-(3-hydroxymyristoyl) glucosamine. The crystal structure of LpxD from *Pseudomonas aeruginosa* has been determined at high resolution (1.3 Å). The crystal belonged to space group *H*3, with unit-cell parameters $a = b = 106.19$, $c = 93.38$ Å, and contained one molecule in the asymmetric unit. The structure was solved by molecular replacement using the known structure of LpxD from *Escherichia coli* (PDB entry 3eh0) as a search model and was refined to R_{work} = 16.4% (R_{free} = 18.5%) using 91 655 reflections. The final protein model includes 355 amino-acid residues (including 16 amino acids from a 20 amino-acid N-terminal His tag), one chloride ion and two ethylene glycol molecules.

1. Introduction

Bacterial resistance to antibiotics, in particular by Gram-negative bacteria, is a growing issue in the clinical setting, with no new agents having been introduced since the 1980s, when carbapenems and fluoroquinolones were first studied (Jacoby, 2005). One organism of particular interest is the Gram-negative bacterium *Pseudomonas aeruginosa*, which is known to cause common and potentially fatal hospital infections and is naturally resistant to a large number of antibiotics (Lockhart *et al.*, 2007). Hence, effective therapeutic strategies that will overcome resistance to *P. aeruginosa* represent a growing unmet medical need. One such strategy is interference with the synthesis of the Gram-negative bacterial cell wall.

The cell wall of Gram-negative bacteria is made up of two membranes. The inner membrane is composed of phospholipid and the outer membrane is composed of phospholipid and lipopolysaccharide (LPS). The ampipathic outer membrane contributes to protection against antibiotics. This membrane is crucial for bacterial survival and is toxic. Specifically, when the LPS cell wall is injected into animals it causes severe sepsis, intravascular coagulation and multiple organ failure (Esmon, 2000). LPS is composed of three components: the O-antigen, which is the surface-exposed linear polysaccharide composed of 50–100 repeating saccharide units, the core oligosaccharide, which most often contains a branched 3-deoxy-D-*manno*-oct-2-ulosonic acid (KDO), and lipid A, which is a phosphorylated glucosamine disaccharide with multiple fatty acids attached *via* ester and amide bonds. It is the lipid A component that is primarily responsible for the macrophage-activating endotoxic activity of LPS (Raetz & Whitfield, 2002).

The first three enzymes responsible for Gram-negative bacterial cell-wall synthesis, LpxA, LpxC and LpxD, are all present as single copies and are essential for bacterial viability. These enzymes are conserved across class A, B and C pathogens and are potential drug targets for the treatment of *P. aeruginosa* and other Gram-negative infections (Raetz, 1990; Raetz & Whitfield, 2002). In *P. aeruginosa* LpxD catalyzes the third step in LPS biosynthesis, transferring a 3-hydroxydecanoyl moiety from acyl carrier protein (ACP) to UDP-3-*O*-(3-hydroxydecanoyl) glucosamine. However, the length of the fatty acid involved in this reaction varies with species. While in

Table 1
Crystal and refinement parameters for LpxD from *P. aeruginosa*.

Values in parentheses are for the highest resolution shell.

Data processing	
Wavelength (Å)	1.0
Unit-cell parameters (Å)	$a = b = 106.19$, $c = 93.38$
Space group	*H*3
Resolution range (Å)	26.85–1.30
No. of observations	873265
No. of unique reflections	96539
Data completeness (%)	99.9 (100)
R_{merge}	0.078 (0.644)
$R_{p.i.m}$	0.027 (0.227)
$\langle I/\sigma(I)\rangle$	14.1 (3.2)
Multiplicity	9.0 (8.9)
Refinement	
Resolution range (Å)	26.85–1.30
No. of observations	91655
No. of protein atoms	2661
No. of ligand and water atoms	455
Mean protein *B* factor (Å^2)	14.05
R_{work}	0.164
R_{free}	0.185
R.m.s.d. bond lengths (Å)	0.007
R.m.s.d. bond angles (°)	1.171
R.m.s.d. *B* factors (Å^2)	
Main-chain bond-related	0.996
Main-chain angle-related	1.538
Side-chain bond-related	1.831
Side-chain angle-related	2.842

P. aeruginosa the reaction begins with *R*-3-hydroxydecanoyl-ACP, the *Escherichia coli* enzyme is specific for the myristic acid form and the *Chlamydia trachomatis* enzyme is specific for the arachidic acid form. Crystal structures of both the *E. coli* and *C. trachomatis* LpxD proteins have been previously solved and are compared with the *P. aeruginosa* structure in this report.

2. Materials and methods

2.1. Cloning and expression

LpxD was amplified with an *Nde*I/*Xho*I restriction site from *P. aeruginosa* genomic DNA using the primers TATATACATATGAGTACCTTGTCCTACACC and TATATACTCGAGTCACGCATCAGATGAAG. Clones were sequence-verified and positive clones were transformed into *E. coli* BL21 (DE3) cells.

2.2. Purification

Cells containing the target plasmid were grown at 310 K until the OD_{600} reached 0.6. The cells were induced with 1 m*M* IPTG at 298 K overnight, harvested and stored at 193 K. Cell pellets was lysed in 50 m*M* Tris pH 7.8, 500 m*M* NaCl, 10% glycerol and 20 m*M* imidazole (lysis buffer). The suspension was sonicated on ice for 1 min at 70% output. The clarified supernatant was loaded onto Ni^{2+}-charged IMAC. Unbound protein was washed out with lysis buffer. The target protein was eluted using a linear gradient from 20 to 250 m*M* imidazole. Elution fractions containing target protein were further purified on a size-exclusion column in 10 m*M* Tris pH 8, 500 m*M* NaCl and 1 m*M* DTT. Monomeric LpxD was then concentrated to 15 mg ml^{-1}.

2.3. Crystallization and data collection

The protein sample was incubated with 50 m*M* uridine diphosphate-*N*-acetylglucosamine (UDP-GlcNac) on ice for 1 h. Crystals of *P. aeruginosa* LpxD including an N-terminal His_6 tag were obtained using the hanging-drop vapor-diffusion method by mixing 2 µl 15 mg ml^{-1} protein solution (in 10 m*M* Tris–HCl pH 8.0 containing 1 m*M* DTT and 500 m*M* NaCl) with 2 µl 100 m*M* Tris pH 8.5, 1.5 *M* lithium sulfate at 293 K. Diffracting crystals appeared within 3–5 d and grew to ∼0.4 mm in length. Similar crystals were also obtained in the absence of UDP-GlcNac. Prior to data collection, crystals were transferred into a cryoprotectant solution consisting of 20%(*v*/*v*) ethylene glycol in crystallization buffer and then flash-frozen in liquid nitrogen.

Diffraction data were collected at a wavelength of 1.0 Å using an ADSC Q315 CCD detector array on beamline 5.0.2 at the Advanced Light Source, Berkeley, California, USA. The crystals diffracted to 1.3 Å resolution and were indexed in space group *H*3, with unit-cell parameters $a = b = 106.19$, $c = 93.38$ Å. A set of 300 consecutive images in 1° increments were measured.

2.4. Structure solution and refinement

Data were indexed, integrated, scaled and merged (Table 1) using the programs *MOSFLM* and *SCALA* from *CCP*4 (Winn *et al.*, 2011). The structure was solved by molecular replacement with *MOLREP* (Vagin & Teplyakov, 2010) using the PDB entry for LpxD from *E. coli* (PDB entry 3eh0; Bartling & Raetz, 2009) as the search model. The

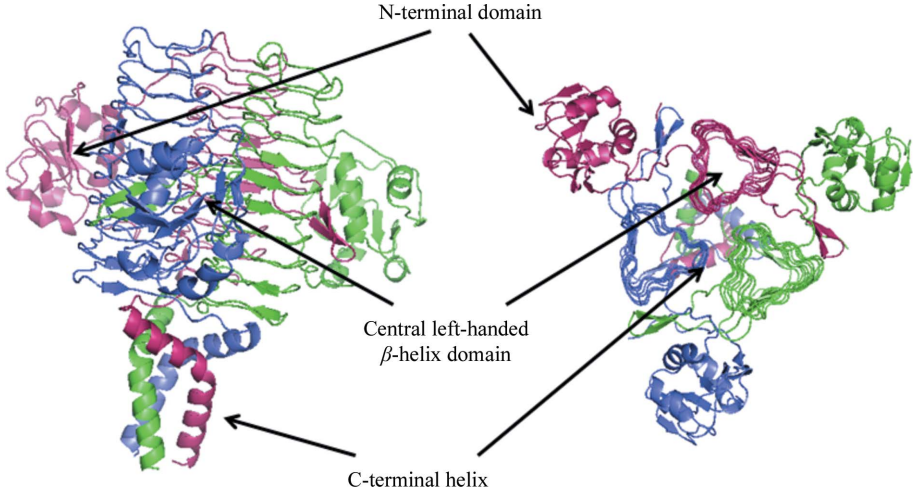

Figure 1
Orthogonal views of the trimeric biological assembly of LpxD from *P. aeruginosa* generated by the application of symmetry operators in the crystal. The three copies of the protein are colored purple, green and blue, respectively. These images were rendered using *PyMOL* (DeLano, 2002).

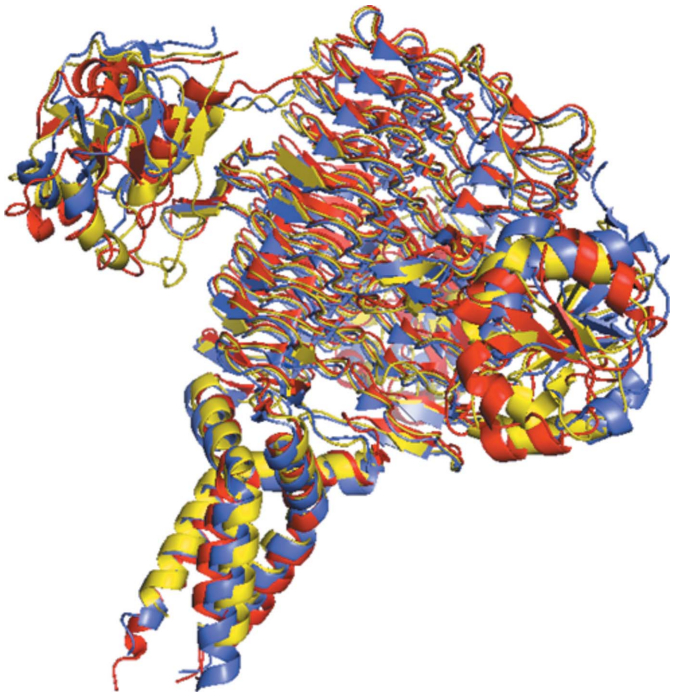

Figure 2
Superposition of the structures of apo crystal forms of LpxD from *E. coli* (PDB entry 3eh0; blue ribbon) and *C. trachomatis* (PDB entry 2iua; red ribbon) onto the present structure from *P. aeruginosa* (yellow ribbon). The tag sequence in the structure from *P. aeruginosa* has been omitted from this figure.

solution was consistent with the expectation of one molecule in the crystal asymmetric unit. Interactive model refitting and molecular-graphics analysis were performed using the *MIFit* software (http://code.google.com/p/mifit/). Reciprocal-space refinement was performed using *REFMAC*5 (Murshudov *et al.*, 2011). Model rebuilding consisted primarily of sequence adjustment to the *P. aeruginosa* species and retracing the N-terminal domain (amino acids 2–96), which differed from the search model to an extent that was not correctable by automated refinement. The final protein model (Table 1) contained 339 amino acids, corresponding to residues 2–340, in an unbroken chain trace. In addition, electron density for 16 amino acids from the 20-amino-acid N-terminal His tag was visible and was fitted. One chlorine ion was identified on the basis of a 7σ feature in an anomalous difference map, an excessively low temperature factor when the density was initially fitted as a water molecule and a location that was consistent with a positively charged environment. Two density features were fitted by ethylene glycol molecules and 446 ordered water sites were identified. The occupancies of water molecules were reduced to less than unity if the water sites were on special positions, to resolve conflicts with partially occupied side chains and, in a few cases, in order to represent highly elongated solvent-density features. The structure refinement used all available structure-factor data with the 'mask' bulk-solvent model and 5% of reflections reserved for cross-validation tests. Individual anisotropic temperature factors were introduced in the final stages of the refinement, resulting in parallel falls in $R_{\rm work}$ and $R_{\rm free}$ of ∼2%. In addition to visual inspection, model quality was continuously assessed during the refinement *via* an automated battery of tests implemented and collected *via* the *MIFit* refinement interface, which included checks on standard protein covalent geometry, flags for *cis*-peptides, checks on short van der Waals contacts, abnormal φ–ψ angles (Lovell *et al.*, 2003) and abnormal side-chain rotamers and flags for significant difference density features overlapping the protein. The conformations of the three amino acids listed as lying outside the expected range in the φ–ψ plots defined by Kleywegt & Jones (1996) are supported by strong electron density.

Table 2
Structural comparisons of LpxD from *P. aeruginosa* with those from *E. coli* and *C. trachomatis*.

Independent overlays were performed using structurally related C$^{\alpha}$ atoms in the N-terminal and central domains of the unique *P. aeruginosa* protein molecule with all three copies of the protein in the crystals of the *E. coli* and *C. trachomatis* proteins.

Species	PDB entry	Resolution (Å)	R.m.s.d., N-terminal domain (Å)	R.m.s.d., central domain (Å)
E. coli	3eh0	2.6	1.43, 1.38, 1.42	0.69, 0.74, 0.80
C. trachomatis	2iua	2.7	1.54, 1.05, 1.14	0.68, 0.67, 0.72

3. Results and discussion

3.1. Protein assembly and domain structure

The active biological assembly of LpxD is believed to be a trimer and the available three-dimensional structures from both *E. coli* (PDB entry 3eh0; Bartling & Raetz, 2009) and *C. trachomatis* (PDB entries 2iua, 2iu8 and 2iu9; Buetow *et al.*, 2007) contain three protein copies in the crystal asymmetric unit. In the crystal structure from *P. aeruginosa* a comparable trimer is generated by crystallographic symmetry operators (Fig. 1).

The characteristic LpxD domain architecture, consisting of an N-terminal domain (amino acids 2–95), a left-handed β-helix central domain containing many short parallel β-sheet segments wrapping through consecutive triangular sections (amino acids 101–305) and a C-terminal helix (amino acids 312–340), is similar to that seen in the LpxD structures from *E. coli* and *C. trachomatis*. As might be anticipated from the interwoven network of stabilizing hydrogen bonds, the central domain is the most ordered region of the *P. aeruginosa* LpxD structure, with average *B* factors for main-chain/side-chain atoms of 10.8/13.1 Å^2, compared with 14.7/16.5 Å^2 for the N-terminal domain and 20.0/22.1 Å^2 for the C-terminal helix.

Superpositions of the structure from *P. aeruginosa* onto apo crystal forms of LpxD from *E. coli* (PDB entry 3eh0) and *C. trachomatis* (PDB entry 2iua) using the C$^{\alpha}$ atoms in the central domain demonstrates a high degree of structure conservation in this region (Fig. 2). When C$^{\alpha}$ atoms from amino acids 101–305 in the present structure are independently superimposed onto equivalent atoms in the three copies of the *E. coli* protein the r.m.s. deviations between these sets of atoms are all ∼0.75 Å (Table 2). Similarly, when amino acids 101–189 and 193–305 (with the chain break being introduced to eliminate a dissimilar region around a point deletion in the *C. trachomatis* protein) are superimposed onto the three copies of the protein in the *C. trachomatis* crystal structure the r.m.s. deviations between equivalent C$^{\alpha}$ atoms are all ∼0.7 Å.

Some dissimilarity in the relative positions of the N-terminal domain and the central domain across species is apparent from the global comparisons outlined above (Fig. 2). In addition, an independent superposition of amino acids 5–95 from the *P. aeruginosa* structure onto the three structures from *E. coli* gives r.m.s. deviations between equivalent C$^{\alpha}$ atoms of ∼1.4 Å (Table 2), indicating that there are also somewhat greater differences within the N-terminal domain than within the central domain. Meaningful overlays of the N-terminal domain from *P. aeruginosa* onto the protein from *C. trachomatis* are complicated by the need to account for the shorter

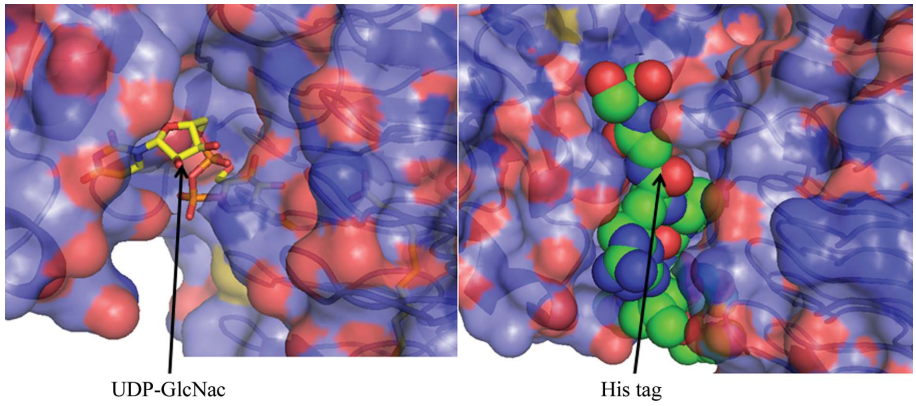

Figure 3
Space-filling views of the region containing the N-terminal tag sequence in the structure from *P. aeruginosa* (right) and UDP-GlcNac binding in a structure from *C. trachomatis* (PDB entry 2iu8, left).

sequence for *C. trachomatis* owing to amino-acid deletions at multiple points; a limited overlay over amino acids equivalent to 5–60 gives r.m.s. deviations between equivalent C^{α} atoms of 1.1–1.5 Å, with the remainder of the structure in this domain containing regions of varying degrees of similarity across the deletion points.

The LpxD structures from *E. coli* and *C. trachomatis* differ in the connectivity of the C-terminal three-helix bundle that is formed from the trimeric assembly. The connectivity in the *P. aeruginosa* structure is the same as that in the *E. coli* structure (Fig. 2).

3.2. Ligand-binding sites

The *P. aeruginosa* LpxD crystal structure was solved without identifying the uridine diphosphate-*N*-acetylglucosamine (UDP-GlcNac) molecule that was contained in two of the crystal structures solved from *C. trachomatis* (PDB entries 2iu8 and 2iu9; Buetow *et al.*, 2007). It does not appear likely that UDP-GlcNac binding is possible in this crystal form of the *P. aeruginosa* protein because the site is partially occluded by an N-terminal His tag (Fig. 3). The tag extends from a neighboring protein molecule (*i.e.* one that is not part of the LpxD trimer) in the crystal and winds through part of the UDP-GlcNac site. However, since the structures from *C. trachomatis* both with (PDB entries 2iu8 and 2iu9) and without (PDB entry 2iua) UDP-GlcNac indicate that there is only a minor change in the local conformation of one of the two proteins involved in UDP-GlcNac binding, this apo structure of *P. aeruginosa* LpxD is probably very similar to the UDP-GlcNac-bound form.

The available *C. trachomatis* LpxD structures also include several palmitic acid molecules bound within crevices between the central domains of the protein molecules in the trimer. Palmitic acid was not included in the crystallization conditions for our structure, but we have identified two bound diethylene glycol molecules in comparable regions, perhaps indicating the hydrophobic nature of this environment.

4. Conclusions

The structure of LpxD from *P. aeruginosa* has been solved at significantly higher resolution than other available LpxD structures in the PDB. This crystal structure may be stabilized by a 20-amino-acid N-terminal His tag, which includes 16 visible amino acids that interact with adjacent protein molecules in the crystal cell. The largest differences between this crystal structure and the previously known LpxD structures from *E. coli* and *C. trachomatis* are in the relative orientation of the central domain to the loosely connected C-terminal domain and within the chain trace of the N-terminal domain.

The Berkeley Center for Structural Biology is supported in part by the National Institutes of Health, National Institute of General Medical Sciences and the Howard Hughes Medical Institute. The Advanced Light Source is supported by the Director, Office of Basic Energy Sciences of the US Department of Energy under Contract No. DE-AC02-05CH11231.

References

Bartling, C. M. & Raetz, C. R. (2009). *Biochemistry*, **48**, 8672–8683.
Buetow, L., Smith, T. K., Dawson, A., Fyffe, S. & Hunter, W. N. (2007). *Proc. Natl Acad. Sci. USA*, **104**, 4321–4326.
DeLano, W. L. (2002). *PyMOL*. http://www.pymol.org/.
Esmon, C. T. (2000). *Biochim. Biophys. Acta*, **1477**, 349–360.
Jacoby, G. A. (2005). *Clin. Infect. Dis.* **41**, S120–S126.
Kleywegt, G. J. & Jones, T. A. (1996). *Structure*, **4**, 1395–1400.
Lockhart, S. R., Abramson, M. A., Beekmann, S. E., Gallagher, G., Riedel, S., Diekema, D. J., Quinn, J. P. & Doern, G. V. (2007). *J. Clin. Microbiol.* **45**, 3352–3359.
Lovell, S. C., Davis, I. W., Arendall, W. B., de Bakker, P. I., Word, J. M., Prisant, M. G., Richardson, J. S. & Richardson, D. C. (2003). *Proteins*, **50**, 437–450.
Murshudov, G. N., Skubák, P., Lebedev, A. A., Pannu, N. S., Steiner, R. A., Nicholls, R. A., Winn, M. D., Long, F. & Vagin, A. A. (2011). *Acta Cryst.* D**67**, 355–367.
Raetz, C. R. (1990). *Annu. Rev. Biochem.* **59**, 129–170.
Raetz, C. R. & Whitfield, C. (2002). *Annu. Rev. Biochem.* **71**, 635–700.
Vagin, A. & Teplyakov, A. (2010). *Acta Cryst.* D**66**, 22–25.
Winn, M. D. *et al.* (2011). *Acta Cryst.* D**67**, 235–242.